Rutherford Backscattering Spectroscopy Study of $TiO_2/Cu_{1.8}S$ Nanocomposites Obtained by Atomic Layer Deposition

Liesbeth Reijnen,*,† Bas Feddes,‡ Arjan M. Vredenberg,§ Joop Schoonman,† and Albert Goossens†

Laboratory for Inorganic Chemistry, Faculty of Applied Sciences, Delft University of Technology, 2628 BL Delft, The Netherlands, Department of Biomaterials, University of Nijmegen, P.O. Box 9101, 6500 HB Nijmegen, The Netherlands, and Section Interface Physics, Debye Institute, Utrecht University, P.O. Box 80.000, 3508 TA Utrecht, The Netherlands

Received: November 28, 2003; In Final Form: March 30, 2004

A new approach to solar cell design is the use of nanostructured heterojunctions of inorganic materials such as n-type TiO_2 and p-type $Cu_{1.8}S$. A major challenge is the deposition of the p-type material inside an n-type nanoporous matrix. In this paper the deposition of $Cu_{1.8}S$ with atomic layer deposition (ALD) inside nanocrystalline (nc)-TiO_2 is presented. The growth of $Cu_{1.8}S$ inside nc-TiO_2 is studied with Rutherford backscattering. Uniform films of $Cu_{1.8}S$ can be deposited inside nc-TiO_2 consisting of 25 nm sized particles as deep as 3 μm, which is sufficient for solar cell applications. Long $Cu(thd)_2$ pulse times lead to a lower infiltration depth, because decomposion of $Cu(thd)_2$ clogs the pores. This indicates that the ALD process using these precursors is not ideal.

Introduction

The growing interest in the large-scale utilization of solar energy calls for newly designed, cheap, and efficient solar cells. Nanoporous structures are of interest, because the enhanced surface area boosts the light absorbing capacity of the cells. Furthermore, nanostructured electrodes reduce the path that photoexcited electrons and holes must travel toward the p−n junction within their lifetime, allowing for a relatively large tolerance for impurities. Excellent use of this concept is made in dye-sensitized solar cells[1] and in solid-state devices using both inorganic[2−4] and organic[5] hole conductors. Recently, a new approach, the extremely thin absorber (ETA) solar cell has been introduced, in which an inorganic absorber between the electron and hole conductor is present. Up to now mainly TiO_2 has been used as the electron conductor, whereas CdTe[6] and $CuInS_2$[7,8] have been used as inorganic absorber films.

A major challenge in the fabrication of this type of solar cell is the deposition of the inorganic absorber film or the inorganic hole conductor inside the pores of a nanoporous matrix. Most commonly used deposition techniques, like thermal evaporation, spray pyrolysis, or reactive sputtering, are so-called line-of-sight techniques and are therefore not suitable for deposition inside pores. Other techniques, like chemical bath deposition and chemical vapor deposition, have the risk of clogging the pores, which limits the infiltration and leads to the formation of voids. Sequential methods such as Succesive Ion Layer Adsorption and Reaction (SILAR) and ion layer gas reaction (ILGAR) can successfully deposit inside pores, but the use of liquid solutions makes these processes time consuming.[8] In SILAR, cluster formation of cations, leading to clogging of pores, has been reported,[8] whereas in ILGAR, the uniformity of the film depends on the material being deposited.[6]

Hence, gas-phase synthesis by atomic layer deposition (ALD), also known as atomic layer chemical vapor deposition (ALCVD) or atomic layer epitaxy (ALE), is an attractive alternative. ALD, developed by Suntola in 1977,[9] uses an alternating precursor supply to ensure layer-by-layer growth. It has proven to be well suited for the deposition of high-quality films with excellent conformity and large area uniformity. Up to now, uniform deposition of Al_2O_3[10] and SiO_2[11] on 10 μm agglomerates of BN particles has been achieved, as well as reduction of the pore diameter of alumina tubular membranes from about 5 nm to 0.5−1 nm for a 20 nm thin film.[12,13] Uniform deposition of HfO_2 films deposited by ALD into 7 μm deep and 0.1 to 0.2 μm wide trenches has been achieved recently,[14,15] and deposition of active catalyst materials on porous high surface area materials has been studied extensively.[16−19] Porous high surface area materials have also been used in the study of adsorption-controlled growth through saturated surface reactions by Haukka et al.,[20] but no details on the substrates are given.

In previous papers we have reported on the deposition of p-type photoactive $Cu_{1.8}S$ by ALD, using $Cu(thd)_2$ and H_2S as the precursors and flat TiO_2 films as the substrate.[21] We have shown that flat film $TiO_2/Cu_{1.8}S$ devices yield a moderate photoresponse.[22] This approach is now extended to the ALD growth of $Cu_{1.8}S$ inside nc-TiO_2 substrates. Key questions are whether the $Cu_{1.8}S$ actually grows inside the nc-TiO_2 and whether the deposited film is uniform throughout the nc-TiO_2 film. A technique commonly used to obtain depth profiles of different elements in a nondestructive way, is Rutherford backscattering spectroscopy (RBS).[23−25] Apart from depth profiling of different elements, it has also been used to determine the diffusion of nanosized spheres in a polymer matrix.[26] Therefore, RBS is a suitable technique to study the growth of $Cu_{1.8}S$ inside nc-TiO_2, which is the topic of the present study.

† Delft University of Technology.
‡ University of Nijmegen.
§ Utrecht University.

10.1021/jp037641b CCC: $27.50
Published on Web 06/09/2004

Experimental Aspects

nc-TiO_2 electrodes were prepared by doctor blading using pastes with four different particle sizes, i.e., 50 nm (Screen Paste, Courtesy of ECN), 25 nm (P25 Degussa), 15 nm (T Solaronics), and 9 nm (HT Solaronics) on Corning glass substrates. After doctor blading, the substrates were dried for 1 h and subsequently annealed for 2 h at 450 °C in ambient atmosphere. The resulting nc-TiO_2 films were around 4 μm thick.

The $Cu_{1.8}S$ films were deposited inside the nc-TiO_2 electrodes in a home-built ALD reactor. The details of this reactor and the process have been published elsewhere.[15] Copper dimethylheptadione ($Cu(thd)_2$) (Strem Chemicals) and H_2S (4.8 Hoekloos) have been used as the precursors and nitrogen as the carrier and purge gas. $Cu(thd)_2$ was evaporated at 117 °C in a quartz boat and subsequently transported to the reactor chamber using a 25 sccm nitrogen flow. Films were grown using typically a 6 s $Cu(thd)_2$ pulse, a 3 s H_2S pulse, and 3 s purge pulses in between. The number of cycles and the deposition temperature were kept constant at 1500 cycles and 200 °C, respectively. The pressure in the reactor was 2 mbar. After deposition the reactor was cooled under an 10:1 N_2:H_2S flow at atmospheric pressure.

After deposition the TiO_2/$Cu_{1.8}S$ interpenetrating networks were characterized using Rutherford backscattering. These measurements were performed with a 2.4 MeV beam of $^4He^+$ particles. The projectiles hit the sample under normal incidence. Two detectors were positioned at an angle of 120° and at an angle of 170°. The depth profiles of the elements were extracted from the data using a simulation program (NDF, developed by Barradas et al.[27]). To convert the atomic density scale to a depth scale, the density of nc-TiO_2 must be known. The density of bulk TiO_2 is 3.84 g/cm^3 and the porosity of nc-TiO_2 prepared by doctor blading is generally 50% to 65%.[28] When we conservatively assume that the porosity is 50%, the density of the nc-TiO_2 is found to be 1.92 g/cm^3. Scanning electron microscope images of cross sections of nc-TiO_2 made by doctor blading show that the thickness and weight of these films are consistent with this density.

The crystalline phase of the $Cu_{1.8}S$ films has been determined by X-ray diffraction (Bruker D8 Advance Diffractometer) and the morphology of the matrix has been studied with a scanning electron microscope (Philips, XL30).

Results

The ALD of Cu_xS on flat film substrates has been described in detail elsewhere,[21] but some relevant aspects will be summarized here. Two different crystalline phases are obtained. At temperatures below 175 °C a simple exchange reaction between $Cu(thd)_2$ and H_2S leads to the deposition of CuS. The complete $Cu(thd)_2$ molecule adsorbs to the substrate surface. During the H_2S pulse CuS is formed while H(thd) is released as a reaction product. In this regime the reaction between $Cu(thd)_2$ and the substrate is self-limiting and ideal ALD growth is obtained. Above 175 °C $Cu_{1.8}S$ is deposited, because $Cu(thd)_2$ becomes thermally unstable at this temperature. $Cu(thd)_2$ decomposes slowly when adsorbed at the surface. The Cu^{2+} reduces to Cu^+ while releasing one of its thd ligands or parts thereof. The other thd ligand is removed during the H_2S pulse. Consequently, the self-limiting surface reaction between $Cu(thd)_2$ and the substrate is lost but because the decomposition rate of $Cu(thd)_2$ is low, smooth uniform films can be obtained for reaction temperatures below 280 °C and moderate $Cu(thd)_2$ pulse times.

The thermal instability of $Cu(thd)_2$ at the deposition temperature and the consequential lack of complete self-limitation implies that this process does not meet all the criteria for growth on highly structured substrates, as mentioned by Haukka et al.[14] But because the decomposition rate is low, it is still possible to obtain uniform deposition of $Cu_{1.8}S$ inside nc-TiO_2.

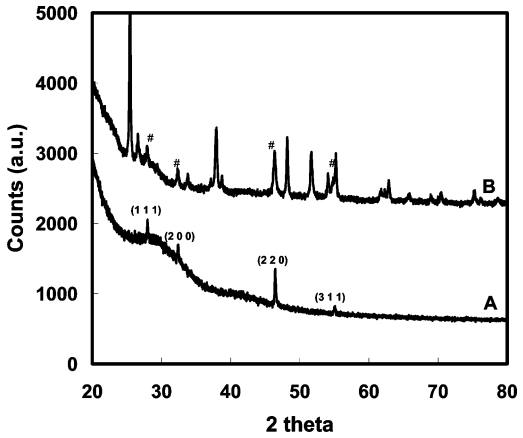

Figure 1. X-ray diffraction patterns of $Cu_{1.8}S$ on Corning glass (A) and infiltrated in a TiO_2 matrix (B). # = $Cu_{1.8}S$ peaks; other peaks can be assigned to either TiO_2 or the SnO_2:F substrate.

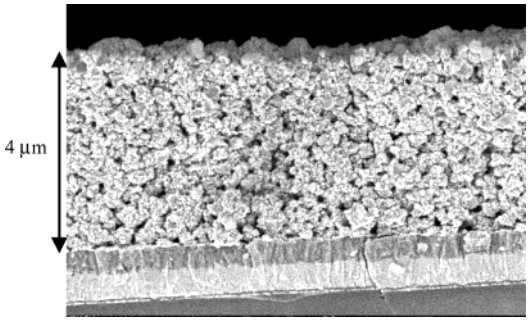

Figure 2. Micrograph of a cross section of a 4 μm TiO_2/$Cu_{1.8}S$ film. $Cu_{1.8}S$ is present inside the TiO_2 film consisting of 50 nm particles.

Figure 1 shows X-ray diffraction patterns, comparing a $Cu_{1.8}S$ film deposited on Corning glass and inside nc-TiO_2. The same diffraction angles are found for both cases and for $Cu_{1.8}S$ deposited on flat TiO_2 (not shown), indicating that films deposited on glass and (nc-)TiO_2 substrates have the same phase composition. A cross section of a 4 μm thick nc-TiO_2 film consisting of 50 nm particles of TiO_2 covered with $Cu_{1.8}S$ is shown in Figure 2. Although this micrograph shows that the morphology is uniform across the film, it does not imply that there is uniform deposition of $Cu_{1.8}S$ throughout the nc-TiO_2 film. To obtain an accurate depth profile, Rutherford backscattering spectroscopy (RBS) measurements have been performed. An example of measurement data from the two detectors is shown in Figure 3. Fits to these data sets along with the surface channels for detector A for all four elements are also included. Because RBS is best suited for the analysis of heavy elements in the presence of a relatively light element matrix[23] and copper and titanium are heavy compared to oxygen and sulfur, it is not possible to obtain accurate results for the concentration of oxygen and sulfur. Therefore, only the copper depth profile inside the TiO_2 matrix has been determined, with the Cu/S ratio set to 1.8. Because XRD only shows the $Cu_{1.8}S$ phase, it is safe to assume that the determined copper profile is exclusively related to the presence of $Cu_{1.8}S$. Likewise, the titanium concentration is constant throughout the film, the amount of titanium found can thus be used to determine the thickness of the nc-TiO_2 film.

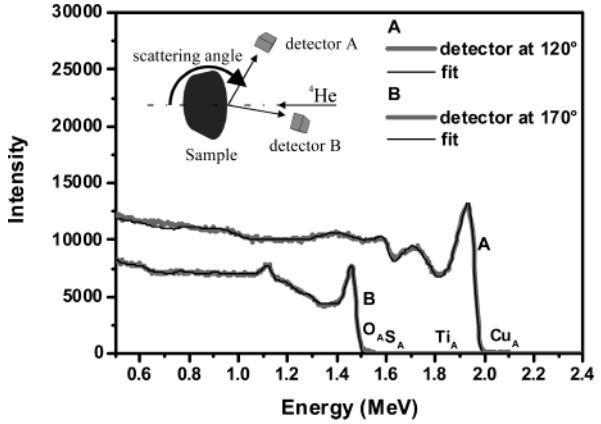

Figure 3. Rutherford backscattering spectroscopy measurement along with obtained simulations and surface channels

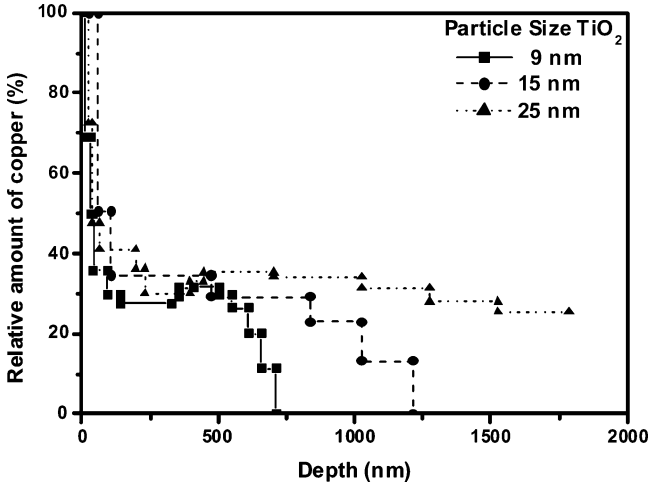

Figure 4. Influence of the particle size on the infiltration depth of copper. The amount of $Cu_{1.8}S$ is scaled to 100% at the surface of the film.

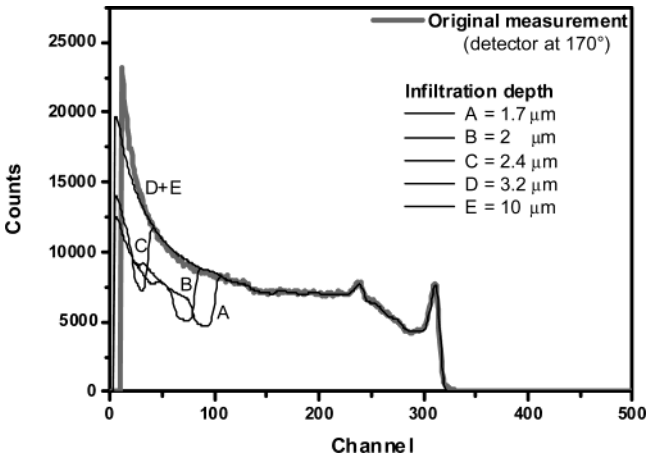

Figure 5. Rutherford backscattering spectroscopy measurement along with obtained simulations for different penetration depths of copper.

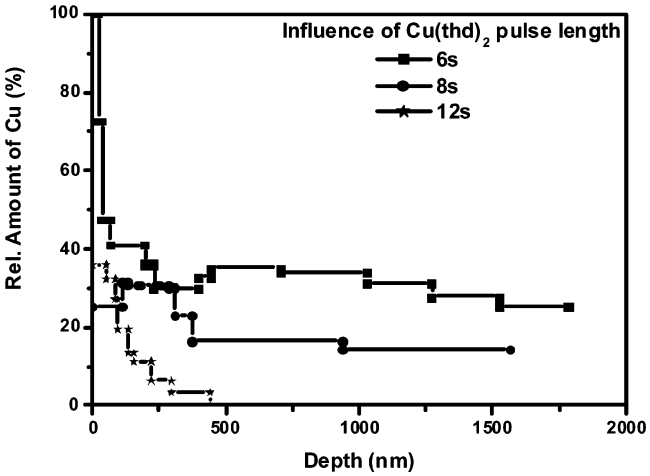

Figure 6. Influence of the $Cu(thd)_2$ pulse time on the infiltration depth of copper for a TiO_2 matrix consisting of 25 nm particles.

Influence of Particle Size. The influence of the particle size on the copper profile along the cross section of the TiO_2 matrix is shown in Figure 4. The amount of copper is scaled to 100% at the surface of the film corresponding to a pure $Cu_{1.8}S$ film on top of the nc-TiO_2. The initial strong decrease in the copper content present in most of the films is, therefore, due to the transition from a pure $Cu_{1.8}S$ film on top of the nc-TiO_2 to the $Cu_{1.8}S$ film inside the nc-TiO_2. It is clear that the $Cu_{1.8}S$ film penetrates deeper into a nc-TiO_2 film consisting of 15 nm particles than in a nc-TiO_2 film of 9 nm particles, whereas the penetration is deepest for the 25 nm particle film. This is as expected because the parameters during film growth are kept the same and the copper precursor, $Cu(thd)_2$, is a relatively large molecule. The diffusion of $Cu(thd)_2$ through a 9 nm particle-film will be slower than the diffusion through a 25 nm particle-film and results in a smaller penetration depth if the same $Cu(thd)_2$ pulse times are used. Also, the total surface area increases with decreasing TiO_2 particle size, meaning that more $Cu(thd)_2$ molecules adsorb and a longer $Cu(thd)_2$ pulse time is needed to cover the whole surface area.

The penetration depth in the 9 nm film is ~750 nm (see Figure 4), and the penetration depth in the 15 nm film is ~1250 nm. Figure 5 shows the data for the 25 nm film from the detector at an angle of 170° combined with simulations corresponding to different penetration depths. It is clear that the simulation becomes better if the penetration is deeper, but at penetration depths higher than 3.2 μm the fit remains the same. This implies that copper penetrates deeper inside the nc-TiO_2 than the maximum probing depth of the RBS measurement and the actual penetration depth in the 25 nm film cannot be obtained but is more than 3.2 μm.

A copper gradient is present in all three films, as can be seen in Figure 4. In an ideal ALD process the surface reactions are self-limiting and reach surface saturation, provided that the pulse times are sufficiently long. A deposition profile is absent in this case. $Cu(thd)_2$ is, however, not stable at 200 °C and the growth rate will depend on the concentration of $Cu(thd)_2$. During the $Cu(thd)_2$ pulse the concentration of $Cu(thd)_2$ in the gas phase will be higher near the surface than near the bottom of the nc-TiO_2 film. The slightly higher concentration will lead to a higher growth rate and, therefore, to a gradient in the thickness of the $Cu_{1.8}S$ film toward the bottom of the nc-TiO_2. As expected, this depletion of copper becomes more pronounced with smaller pore sizes.

Influence of the $Cu(thd)_2$ Pulse Time. The copper concentration as a function of the depth inside the nc-TiO_2, consisting of 25 nm particles, is shown for three different $Cu(thd)_2$ pulse times in Figure 6. For a $Cu(thd)_2$ pulse time of 6 s the copper concentration reveals a pronounced gradient near the surface of the film followed by a slight gradient deeper inside the nc-TiO_2. In the films prepared with a $Cu(thd)_2$ pulse time of 6 and 8 s the actual penetration depth of copper could not be determined due to the detection limit of the RBS technique, but it exceeds 2 μm in both cases. Surprisingly, the film obtained

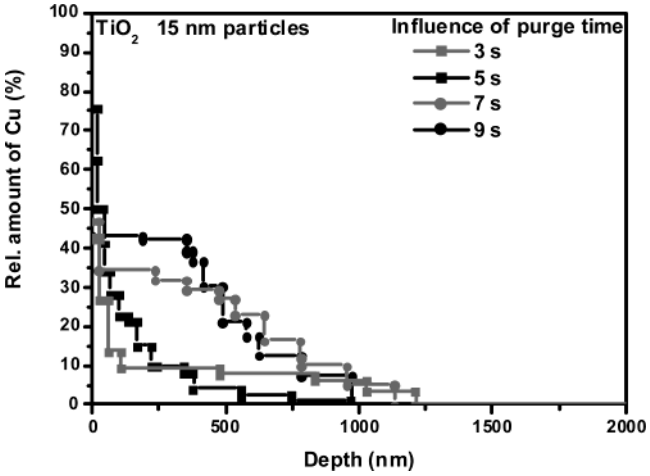

Figure 7. Influence of the purge time after the H_2S pulse on the infiltration depth of copper for a TiO_2 matrix consisting of 15 nm particles.

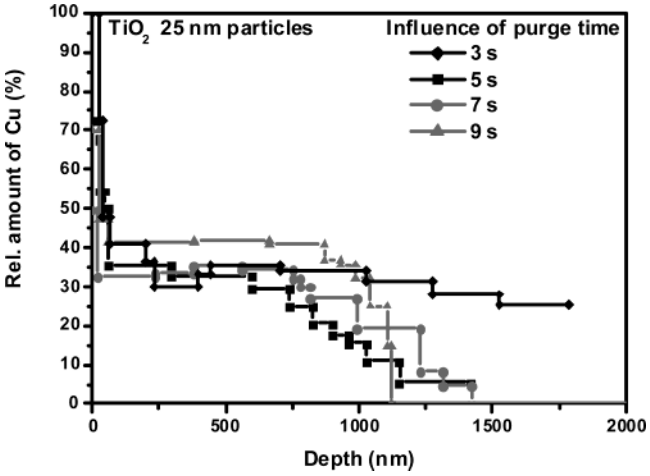

Figure 8. Influence of the purge time after the H_2S pulse on the infiltration depth of copper for a TiO_2 matrix consisting of 25 nm particles.

using a 12 s $Cu(thd)_2$ pulse time shows a very strong gradient and a copper penetration depth of only 500 nm. Apparently, the decomposition of $Cu(thd)_2$ becomes significant at pulse times over 8 s. Significant decomposition leads to a relatively high growth rate during the $Cu(thd)_2$ pulse, which will clog the pores near the surface of the nc-TiO_2 film in the first few cycles. $Cu_{1.8}S$ film growth then occurs on top rather than inside the nc-TiO_2 film.

Influence of Purge Time. Apart from the pulse times of the precursors, the purge times are also important. The purge time needs to be long enough to allow reaction products to diffuse through the matrix and escape from the reaction chamber. In the case of the reaction between $Cu(thd)_2$ and H_2S the purge time after the H_2S pulse is most important, because during the H_2S pulse the thd ligands are removed from the surface.[21] Figure 7 shows the influence of the purge time after the H_2S pulse for the TiO_2 matrix consisting of 15 nm particles. It is clear that the penetration depth ($\pm$1000$-$1200 nm) does not change significantly with increasing purge time, but the amount of copper in the film and the copper profile do. The decreasing amount of copper with decreasing purge time in the area near the surface of the TiO_2 film and the more pronounced copper profile are probably due to the presence of reaction products such as Hthd in the pores, hindering the diffusion of $Cu(thd)_2$ inside the nc-TiO_2 during the next pulse. With longer purge times more reaction products diffuse through the matrix and leave the reaction chamber. Accordingly, fewer reaction products are left inside the matrix and more $Cu(thd)_2$ can react with the surface during the next cycle. The fact that a pronounced copper profile can still be seen when a 9 s purge time is used, indicates that not all reaction products have been removed from the matrix yet and even longer purge times are needed.

If a TiO_2 matrix of 25 nm particles is used, the situation is totally different, as can be seen in Figure 8. A 3 s purge time leads to a relatively small deposition gradient and a penetration depth of over 2 μm, whereas the penetration depth decreases with increasing purge time to about 1400 nm at a purge time of 9 s. The amount of copper near the surface of the film is roughly the same, indicating that in this case reaction products have already been removed from the nc-TiO_2 at a purge time of 3 s. Because no reactants are present and the penetration is deepest when a 3 s purge is used, we expect that the $Cu_{1.8}S$ film changes somewhat during the purge time.

The reason for this is not completely understood, but a known postdeposition treatment to increase the copper content of Cu_xS films is a heat treatment at 200 °C in a nitrogen atmosphere.[29] During this treatment sulfur evaporates from the film, until in the end only copper is left. Experiments performed in our laboratory of Cu_xS films at 200 °C in a nitrogen atmosphere and vacuum also suggest the evaporation of sulfur from the Cu_xS films. Therefore, we conclude that sulfur evaporates from the $Cu_{1.8}S$ film during the purge after the H_2S pulse. The resulting Cu_xS film will again be transformed into $Cu_{1.8}S$ during the next sulfur pulse.

Obviously, more sulfur will evaporate from the film with longer purge times, and it is apparent that the $Cu_{1.8}S$ film loses so much sulfur near the bottom of the nc-TiO_2 at purge times over 3 s that the film breaks down into copper and free sulfur. The result is that $Cu(thd)_2$ is not able to chemisorb at the (copper) surface during the next pulse[30] and film growth ceases. It is, however, not clear why this only happens at the bottom of the nc-TiO_2 and not throughout the whole matrix. After growth the $Cu_{1.8}S$/nc-TiO_2 matrix is cooled under atmospheric pressure and in a N_2/H_2S flow, preventing the film from losing sulfur in this case.

The difference in pore size leads to a difference in behavior between nc-TiO_2 consisting of 15 nm particles and nc-TiO_2 of 25 nm particles. The pores in the latter are larger, and therefore, reaction products are removed from the nc-TiO_2 within 3 s. In the 15 nm particle size nc-TiO_2, the removal of reaction products is slower and the beneficial effect of reaction product removal with longer purge time outweighs the negative effects of the sulfur evaporation, leading to deeper infiltration at longer purge times.

Conclusions

Although the $Cu_{1.8}S$ deposition by ALD using $Cu(thd)_2$ and H_2S as the precursors is not an ideal ALD process, almost uniform deposition of $Cu_{1.8}S$ inside the pores of a TiO_2 matrix can be achieved. Penetration depths in TiO_2 matrixes of 25 nm particles exceed 3 μm, which is sufficient for full absorption in solar cell applications.

Contrary to what is expected in an ideal ALD process, deeper and more uniform infiltration is achieved, if pulse times are limited. At prolonged $Cu(thd)_2$ pulse times clogging of the pores occurs due to the absence of self-limitation. Purge times need to be long enough to ensure the diffusion of reaction products out of the nc-TiO_2. However, at prolonged purge times the

$Cu_{1.8}S$ film nearest to the bottom of the nc-TiO_2 starts to decompose.

References and Notes

(1) O'Regan, B.; Grätzel, M. *Nature* **1991**, *353*, 737.

(2) Tennakone, K.; Kumara, G. R. R. A.; Kumarasinghe, A. R.; Wijayantha, K. G. U.; Sirimanne, P. M. *Semicond. Sci. Technol.* **1995**, *10*, 1689.

(3) O'Regan, B.; Schwartz, D. T.; Zakeeruddin, S. M.; Grätzel, M. *Adv. Mater.* **2000**, *12*, 1263.

(4) Tennakone, K.; Kumara, G. R. R. A.; Wijayantha, K. G. U.; Kottegoda, I. R. M.; Perera, V. P. S.; Aponsu, G. M. L. P. *Semicond. Sci. Technol.* **1998**, *13*, 134.

(5) Bach, U.; Lupo, D.; Comte, P.; Moser, J. E.; Weissörtel, F.; Salbeck, J.; Spreitzer, H.; Grätzel, M. *Nature* **1998**, *395*, 583.

(6) Ernst, K.; Sieber, I.; Neumann-Spallart, M.; Lux-Steiner, M.-Ch.; Könenkamp, R. *Thin Solid Films* **2000**, *361*−*362*, 213.

(7) Kaiser, I.; Ernst, K.; Fischer, Ch.-H. Könenkamp, R.; Rost, C.; Sieber, I.; Lux-Steiner, M. Ch. *Sol. Energy Mater. Sol. Cells* **2001**, *67*, 89.

(8) Möller, J.; Fischer, Ch.-H.; Muffler, H.-J.; Könenkamp, R.; Kaiser, I.; Kelch, C.; Lux-Steiner, M. C. *Thin Solid Films* **2000**, *361*−*362*, 113.

(9) Suntola, T.; Antson, J. *U.S. Pat. 4,058,430* **1977**.

(10) Ferguson, J. D.; Weimer, A. W.; George, S. M. *Thin Solid Films* **2000**, *371*, 95.

(11) Ferguson, J. D.; Weimer, A. W.; George, S. M. *Chem. Mater.* **2000**, *12*, 3472.

(12) Berland, B. S.; Gartland, I. P.; Ott, A. W.; George, S. M. *Chem. Mater.* **1998**, *10*, 3941.

(13) Ott, A. W.; Klaus, J. W.; Johnson, J. M.; George, S. M. *Chem. Mater.* **1997**, *9*, 707.

(14) Gordon, R. G.; Hausmann, D.; Kim, E.; Shepard, J. *Chem. Vap. Dep.* **2003**, *9*, 73.

(15) Hausmann, D.; Becker, J.; Wang, S.; Gordon, R. G. *Science* **2002**, *298*, 402.

(16) Keränen, J.; Guimon, C.; Iiskola, E.; Auroux, A.; Niinistö, L. *Catal. Today* **2003**, *78*, 149.

(17) Puurunen, R. L.; Root, A.; Sarv, P.; Haukka, S.; Iiskola, E. I.; Lindblad, M.; Krause, A. O. I. *Appl. Surf. Sci.* **2000**, *165*, 193.

(18) Lindblad, M.; Haukka, S.; Kytökivi, A.; Lakomaa, E. L.; Rautiainen, A.; Suntola, T. *Appl. Surf. Sci.* **1997**, *121*−*122*, 286.

(19) Lakomaa, E. L. *Appl. Surf. Sci.* **1994**, *75*, 185.

(20) Haukka, S.; Suntola, T. *Interface Sci.* **1997**, *5*, 119.

(21) Reijnen, L.; Meester, B.; Goossens, A.; Schoonman, J. *Chem. Vap. Dep.* **2003**, *9*, 15.

(22) Reijnen, L.; Meester, B.; Goossens, A.; Schoonman, J. *Mater. Sci. Eng. C*, **2002**, *19*, 311.

(23) Markwitz, A.; Matz, W.; Schmidt, B.; Grötzschel, R. *Surf. Interface Anal.* **1998**, *26*, 359.

(24) Markwitz, A. *Nucl. Instrum. Methods Phys. Res. B* **2000**, *161*−*163*, 221.

(25) Feldman, L. C.; Mayer, J. W. *Fundamentals of surface and thin film analysis*; North-Holland: Amsterdam, 1986.

(26) Cole, D. H.; Shull, K. R.; Rehn, L. E.; Baldo, P. M. *Nucl. Instrum. Methods Phys. Res. B* **1998**, *136*−*138*, 283.

(27) Barradas, N. P.; Jeynes, C.; Webb, R. P. *Appl. Phys. Lett.* **1997**, *71*, 291.

(28) van de Lagemaat, J.; Benkstein, K. D.; Frank, A. J. *J. Phys. Chem. B* **2001**, *105*, 12433.

(29) Aperathitis, E.; Bryant, F. J.; Scott, C. G. *Sol. Energy Mater.* **1990**, *20*, 115.

(30) Mårtensson, P.; Carlsson, J.-O. *J. Electrochem. Soc.* **1998**, *145*, 2926.